Effects of low level laser therapy on inflammatory and angiogenic gene expression during the process of bone healing: A *microarray* analysis

Carla Roberta Tim [a,*], Paulo Sérgio Bossini [b], Hueliton Wilian Kido [a], Iran Malavazi [c],
Marcia Regina von Zeska Kress [d], Marcelo Falsarella Carazzolle [e,f],
Nivaldo Antonio Parizotto [a], Ana Cláudia Rennó [b]

[a] Federal University of São Carlos, Department of Physiotherapy, Rod Washington Luis Km 235, São Carlos 13565-905, Brazil
[b] Federal University of São Paulo, Department of Bioscience, Av. Ana Costa 95, Santos 11050-240, Brazil
[c] Federal University of São Carlos, Department of Genetics and Evolution, Rod Washington Luis Km 235, São Carlos 13565-905, Brazil
[d] University of São Paulo, School of Pharmaceutical Sciences of Ribeirão Preto, Department of Clinical Analysis, Toxicological and Bromatological, Av. do Café 95, Ribeirão Preto, Brazil, 14049-900, Brazil
[e] State University of Campinas, Department of Genetics and Evolution, Cidade Universitária Zeferino Vaz, Campinas 13083-970, Brazil
[f] Brazilian National Center for Research in Energy and Materials, Brazilian Biosciences National Laboratory, Giuseppe Máximo Scolfaro 10.000, Campinas 13083-970, Brazil

ARTICLE INFO

ABSTRACT

The process of bone healing as well as the expression of inflammatory and angiogenic genes after low level laser therapy (LLLT) were investigated in an experimental model of bone defects. Sixty Wistar rats were distributed into control group and laser group (830 nm, 30 mW, 2,8 J, 94 seg). Histopathological analysis showed that LLLT was able to modulate the inflammatory process in the area of the bone defect and also to produce an earlier deposition of granulation tissue and newly formed bone tissue. *Microarray* analysis demonstrated that LLLT produced an up-regulation of the genes related to the inflammatory process (MMD, PTGIR, PTGS2, Ptger2, IL1, 1IL6, IL8, IL18) and the angiogenic genes (FGF14, FGF2, ANGPT2, ANGPT4 and PDGFD) at 36 h and 3 days, followed by the decrease of the gene expression on day 7. Immunohistochemical analysis revealed that the subjects that were treated presented a higher expression of COX-2 at 36 h after surgery and an increased VEGF expression on days 3 and 7 after surgery. Our findings indicate that LLLT was efficient on accelerating the development of newly formed bone probably by modulating the inflammatory and angiogenic gene expression as well as COX2 and VEGF immunoexpression during the initial phase of bone healing.

© 2015 Elsevier B.V. All rights reserved.

1. Introduction

Fracture healing is a multistage repair process that involves complex and well-orchestrated steps which are initiated in response to the injury and with the purpose of recovering bone mechanical functions [1,2]. In general, bone tissue has the ability of healing by itself [3]. However, under critical conditions, such as in larger bone defects and fractures with inadequate or interrupted vascularization, a delay in the healing process or even a nonunion may happen [4]. Therefore, innovative clinical approaches such as low-level laser therapy (LLLT) [5,6] have been developed in order to stimulate the bone healing process.

LLLT irradiation stimulates mitochondrial metabolism, which results in an increased expression of adenosine triphosphate (ATP), molecular oxygen production [6] and transcription factors [7]. These effects may increase the synthesis of DNA, RNA and cell-cycle regulatory proteins, therefore stimulating cell proliferation [8,9]. Moreover, LLLT could

modulate the expression of some inflammatory mediators such as interleukin 1β, (IL1β), interleukin 6 (IL6), interleukin 10 (IL10) and tumor necrosis factor α (TNFα) [6,10–12]. Furthermore, it has been demonstrated that LLLT stimulates angiogenesis, which is an essential part of the healing process [13,14]. Based on the effects of LLLT aforementioned, this therapeutic modality has been used to promote wound healing, to accelerate tissue repair and to modulate the inflammatory processes after injuries [15,16]. Furthermore, the effects of LLLT on the process of bone consolidation have been demonstrated and showed an increased osteoblastic activity [17], neoangiogenesis as well as higher newly formed bone deposition at the site of the fracture [15]. In a recent *in vivo* study, Bossini *et al.* [13] observed that LLLT (830 nm) could increase newly formed bone and angiogenesis at the site of the fracture in an experimental model of bone defect in the tibias of rats.

Despite the encouraging data concerning the osteogenic potential of LLLT, the molecular and cellular mechanisms by which this therapy acts on tissues remain unclear [18,19]. Moreover, works describing the effects of LLLT in expression of inflammatory and angiogenic genes in early fracture healing are still scarce. Thus, with the advent of more sophisticated techniques in gene expression analysis (*i.e. microarrays*), it

has become possible to examine the global gene expression and to investigate entire pathways that command biological processes. Therefore, *microarray* is very helpful in identifying possible genes regulated by LLLT during the process of bone healing [20].

In view of the aforementioned information, it was hypothesized that LLLT can regulate the expression of genes involved in the inflammatory process and angiogenesis, which in turn may accelerate the process of bone repair. Thus, the present study aimed to investigate the histological modifications in the bone callus and to study the expression of genes related to the inflammatory process and the formation of new blood vessels after LLLT irradiation in the initial stages of healing.

2. Materials and Methods

2.1. Experimental Design

Sixty male Wistar rats (12 weeks old; weighing ~300 g) were used in this study, which was conducted in accordance with the Guide for Care and Use of Laboratory Animals and approved by the Animal Ethics Committee of the Federal University of São Carlos (010/2011).

Anesthesia was induced by an intra-peritoneal injection of Ketamine (Agener®, 40 mg/kg, IP) and Xylazine (Syntec®, 20 mg/kg, IP). Bilateral bone defects (3.0 mm diameter) were surgically created at the tibia (10 mm distal of the knee joint). In order to do this, the tibia was exposed through a longitudinal incision on the shaved skin, and after that, bone defect was created by using a motorized round drill (BELTEC®, Araraquara-SP, Brazil), under constant physiologic saline solution irrigation. Once the defect had been done, it was packed with sterile cotton gauze to stop bleeding. Thereafter, the cutaneous flap was joined and sutured with resorbable Vicryl® 5–0 (Johnson & Johnson, St. Stevens-Woluwe, Belgium). The animals were divided into 2 groups (n = 30 each group): bone defect control group (CG) (bone defects without any treatment) and bone defect laser irradiated group (LG). In order to minimize post-operative discomfort, the animals received analgesia (i.m., 0,02 mg/kg buprenorfiine — Temgesic; Reckitt Benckiest Healt Care Ltd. Schering-Plow, Hoddesdon, UK) directly after the operation and subcutaneously for 2 days after surgery. Rats were individually euthanized by carbon dioxide asphyxia in different set points (36 h, 3 days and 7 days after surgery).

2.2. Low Level Laser Therapy

A laser (Thera laser, DMC®, São Carlos, Brazil), CW, 830 nm, 0.6 mm beam diameter, 30 mW, 94 s, 2.8 J was used in this study. LLLT sessions were applied immediately after the surgery and repeated every 24 h at two, three and seven days. Treatments were performed by the contact technique, at one point, above the site of the injury.

2.3. Retrieval of Specimens

The right tibias, used for gene expression evaluation (n = 10 per group), were dissected, rapidly frozen in liquid nitrogen and stored in a freezer at −80 °C until *microarray* analysis was carried out. For the histopathological analysis, the left tibias (n = 10 per group), were removed and immediately fixed in 10% formaldehyde (Merck, Darmstadt, Germany) for 24 h, then were decalcified in 4% diamine tetra-acetic acid (EDTA) (Merck, Darmstadt, Germany) and embedded in paraffin blocks. Therefore, thin sections (5 μm) were prepared in the longitudinal plane, using a micrometer (Leica RM-2145, Germany). Afterwards, the laminas were stained with hematoxylin and eosin (H.E stain, Merck, Darmstadt, Germany).

2.4. Histopathological Analysis

A descriptive qualitative histopathological evaluation of the total area of the bone defect was performed by two experienced observers (PB and CT) in a blinded manner, under a light microscope (Olympus, Optical Co. Ltd., Tokyo, Japan) [13,15]. Any changes in the bone defect, such as the presence of blood clots, fibrin, inflammatory processes, granulation tissue, woven bone or even tissues undergoing hyperplastic, metaplastic and/or dysplastic transformation were investigated in each animal.

2.5. RNA Sample Preparation

Total RNA was isolated using the TRIzol® reagent (Invitrogen, Carlsbad, California) according to the manufacturer's instructions. After the RNA isolation, the samples were purified using the illustra RNAspin Mini RNA Kit (GE Healthcare Life Sciences, USA) according to the manufacturer's instructions. The RNA concentrations were determined using a NanoVue spectrophotometer (GE Healthcare Life Sciences, USA). The quality and integrity of the total RNA were evaluated with an Agilent 2100 Bioanalyzer (GE Healthcare Life Sciences, USA) and samples presenting RNA integrity numbered ≥8 were used for cRNA synthesis.

2.6. Microarray Hybridizations

Microarray hybridizations were performed with Agilent Whole Rat Genome *Microarray* 4 × 44 K. The labeling and *microarray* hybridizations were performed by Agilent using Two-Color *Microarray*-Based Gene Expression Analysis (Agilent Technologies, USA). Briefly, for cDNA synthesis and labeling 200 ng of total RNA were used. Afterwards, cDNA was transcribed into cRNA and was labeled using Agilent Low RNA input Fluorescent Linear Amplification Kit (Agilent Technologies, Santa Clara, CA, USA). Then, the labeled cRNA was purified, mixed with hybridization buffer and hybridized to an Agilent Whole Rat Genome *Microarray* 4 × 44 K for 17 h at 65 °C, according to the manufacturer's instructions. After hybridization, *microarrays* were sequentially washed: 1 min at room temperature in GE Wash Buffer 1 (Agilent Technologies, USA) then 1 min at 37 °C in GE Wash Buffer 2 (Agilent Technologies, USA), followed by 10 s in Acetonitrile Wash (Agilent Technologies, USA) and finally 30 s in Stabilization and Drying Solution wash (Agilent Technologies, USA). Afterwards, *microarray* slides were scanned using GenePix® 4000B *microarray* scanner (Molecular Devices, USA) with simultaneously scanning the Cy3 and Cy5 channels at a resolution of 5 μm. Laser was set at 100% and PMT gain was automatically adjusted for each slide using the program GenePix 4000B according to the intensity of the signal in each array.

2.7. Microarray Data Analysis

Microarray data analysis was performed as described by Castro *et al.*, [21]. Data files were generated using Agilent's Feature Extraction Software (version 11.5, Agilent) and the default parameters, which include Lowess based signal normalization. The dye-normalized values generated in the Feature Extraction data files were used to upload the software Express Converter (version 2.1, TM4 available at http://www.tm4.org/utilities.html) which conveniently converts the Agilent file format to MeV (MultiExperiment View) file format compatible to the TM4 softwares for *microarray* analysis (available at http://www.tm4.org/). The MeV files were then uploaded in the MIDAS software where the resulting data were averaged from replicated genes on each array, from three biological replicates, taking a total of 3 intensity data points for each gene. The MeV files generated were then loaded in MeV software where differentially expressed genes were identified using one-class t-test (p > 0.01). Significantly different genes were those whose mean log2 expression ratio over all included samples was statistically different from 0 which indicates the absence of gene modulation.

2.8. Functional Analyses Using Ingenuity Pathways Analysis (IPA) Software

A network analysis was performed using the Ingenuity Pathways Analysis (IPA) (Ingenuity Systems, www.ingenuity.com) algorithm. The lists of differentially expressed genes were entered into the IPA software to explore relevant biological networks and to assess interactions with other genes. A hypothetical global gene interaction network was constructed, showing the most relevant direct and indirect connections of genes found to be regulated under LLLT.

2.9. Quantitative Real-Time Polymerase Chain Reaction (RT-PCR)

RT-PCR was performed to confirm the differential expression results obtained by the *microarray* experiments. Total RNA was extracted and purified using the experimental protocols described above. One microgram of total RNA was reverse-transcribed into cDNA, and followed by RT-PCR amplification using rat gene-specific *primers* (Table 1), which were designed by *Primer*Express Software (Applied Biosystems, Foster City, CA, USA). The optimized PCR conditions were: initial denaturation at 94 °C for 10 min, followed by 40 cycles consisting of denaturation at 94 °C for 15 s, annealing at 60 °C for 1 min, and extension at 72 °C for 45 s, with a final extension step at 72 °C for 2 min. Negative control reactions with no template (deionized water) were also included in each run. For each gene, all samples were amplified simultaneously in duplicate in one assay run. Analysis of relative gene expression was performed using the 2-ΔΔCT method. RPS18 was used as a housekeeping gene to normalize our expression data.

2.10. Immunohistochemistry

After deparaffinization and rehydration in graded ethanol, each specimen was pretreated in a Steamer with buffer Diva Decloaker (Biocare Medical, CA, USA) for 5 min for antigen retrieval. The material was pre-incubated with 0.3% hydrogen peroxide in phosphate-buffered saline (PBS) solution for 30 min in order to inactivate endogenous peroxidase and then blocked with 5% normal goat serum in PBS solution for 20 min. Three sections of each specimen were incubated with anti-cyclooxygenase-2 (COX-2, Cat. n° sc-1747) polyclonal primary antibody and anti-vascular endothelial growth factor (VEGF, Cat. n° sc-1881) polyclonal primary antibody, both at a concentration of 1:200 (Santa Cruz Biotechnology, Santa Cruz, USA). Incubation was performed overnight at 4 °C in refrigerated environment. Afterwards, two washes were done in PBS for 10 min. Then, incubation of the sections was performed making use of biotin conjugated secondary antibody anti-rabbit IgG (Vector Laboratories, Burlingame, CA, USA) at a concentration of 1:200 in PBS for 30 min. The sections were washed twice with PBS followed by the application of preformed avidin biotin complex conjugated to peroxidase (Vector Laboratories, Burlingame, CA, USA) for 30 min. The bound complexes were visible by the application of a 0.05% solution of 3-3′-diaminobenzidine solution and counterstained with Harris hematoxylin. In order to carry out control studies of the antibodies, the serial sections were treated with rabbit IgG (Vector Laboratories, Burlingame, CA, USA) at a concentration of 1:200 instead of the primary antibody. Furthermore, internal positive controls were performed with each staining bath.

Table 1
Real-time PCR *primers*.

Gene	Forward *primer*	Reverse *primer*
RPS18	GTGATCCCCGAGAAGTTTCA	AATGGCAGTGATAGCGAAGG
PTGER2	GAACTGCGAGAGCTCGTCAGTATCTC	CCCCGGCCGTGAACAT
IL1R1	AAGTGGAATGGGTCGGAAATT	TGAAGGGTGTTCCAAAAACTGA
ANGPT4	GGCATCTACTATCCGGTTCATCA	CATGCGTGTGCCATGCAi
PDGFD	TATGCTCATTGGATGCCTTGTC	TGCTGCTATCGGGACACTTTT
FGF2	AAGGATCCCAAGCGGCTCTA	CGGCCGTCTGGATGGA

COX-2 and VEGF immunoexpression was assessed both qualitatively (presence of the immunomarkers) and semi-quantitatively in five pre-determined fields using a light microscopy (Leica Microsystems AG, Wetzlar, Germany) according to a previously described scoring scale ranging from 1 to 4 (1 = absent, 2 = slight, 3 = moderate and 4 = intense) for immunohistochemical analysis [15]. The analysis was performed by 2 observers (PB and CT), in a blinded manner.

2.11. Statistical Analysis

The normality of all variables distribution was verified using Shapiro–Wilk's W test. For immunohistochemical analysis, comparisons among groups were performed using one-way analysis of variance (ANOVA), complemented by Tukey post-test analysis. STATISTICA version 7.0 (data analysis software system — StatSoft Inc.) was used to carry out the statistical analysis. Values of $p < 0.05$ were considered statistically significant.

3. Results

3.1. Histopathological Analysis

Representative histological images of all experimental groups are depicted in Fig. 1.

Thirty-six hours after surgery, histology assessment for CG revealed that the bone defect area was filled with blood clotting and inflammatory tissue, as well as polymorphonuclear cells (Fig. 1A). At the same period, for LG, an intense inflammatory process filled bone defect area. Furthermore, some granulation tissue, mainly at the periphery of the defect, was observed (Fig. 1B). Fig. 1C shows that, 3 days after surgery, in the CG, inflammatory cells still could be observed, especially in the central region of the defect. Moreover, most of the injury area was filled by granulation tissue and immature newly formed bone surrounding the border (Fig. 1C). For LG, some inflammatory cells were still observed. Most all of the defect was filled by granulation tissue and immature newly formed bone at the periphery (Fig. 1D).

On day 7 after surgery, in CG, granulation tissue was present in almost all defect area. Some immature newly formed bone was seen in the peripheral area of the injury (Fig. 1E). At the same period, histological assessment revealed an absence of inflammatory processes in LG. In addition, the bone defects were filled with newly formed bone, with interconnected concentric trabeculae. Areas of granulation tissue still could be observed. (Fig. 1F).

3.2. Microarray Analysis

After sorting through the *microarray* analysis, a total of 5.765 genes modulated by LLLT, in the 3 experimental periods, were identified and organized in a hierarchical cluster.

3.2.1. Functional Network Analysis

Traditional analysis of the *microarray* data by generating a list of regulated genes is not sufficient to understand the functions of the regulated genes and their roles in biological and physiological processes. Therefore, in this study, a reliable new bioinformatics approach, Ingenuity Pathways Analysis (IPA) (Ingenuity, CA) was applied to set up a potential network which is based on the regulated genes in order to identify the molecular events and further unveil the molecular mechanisms regulating the processes of LLLT effects in bone. In order to start building networks, IPA queries the Ingenuity Pathways Knowledge Base for interactions between the regulated genes and the genes stored in the database. The networks were identified and ranked according to the score p-score $= -\log10$ (p-value). The score takes into account the number of Network Eligible Molecules in the network and its size, as well as the total number of Network Eligible Molecules analyzed and the total number of
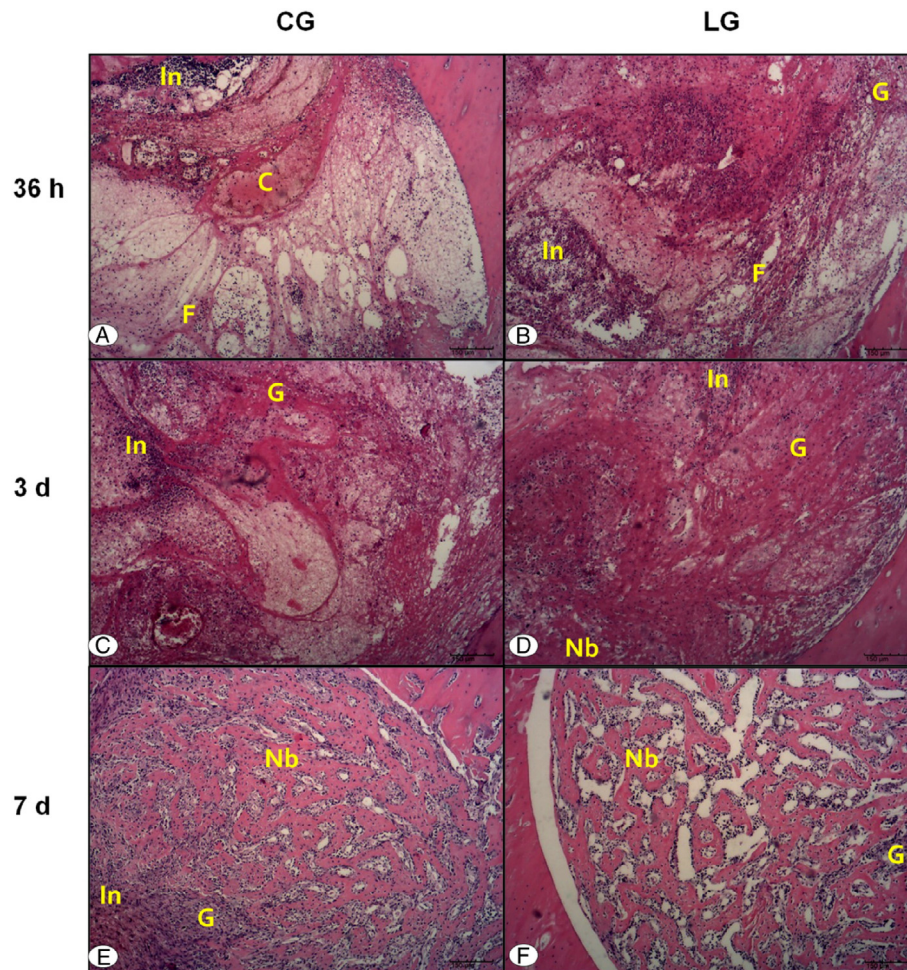
Fig. 1. Representative histological sections of experimental groups showing newly formed bone (Nb), fibrin (F), granulation tissue (G), inflammatory infiltrate (In), and blood clot (C). (Hematoxylin and eosin stain; scale bar = 150 μm).

molecules in the Ingenuity Knowledge Base, which could potentially be included in networks. A score >3 (p < 0.001) indicates a >99.9% confidence that a gene network was not generated by chance alone. Furthermore, the IPA score can be interpreted as the probability of getting a network containing at least the same number of Network Eligible molecules by chance when randomly picking genes that can be in networks from the Ingenuity Knowledge Base. This study showed that LLLT was capable of inducing several networks that may be involved in bone healing. In particular, networks associated to inflammatory responses, connective tissue development and skeletal and muscular system activity were investigated (Table 2).

After merging the networks listed in Table 2, several canonical pathways which were based on their functional annotations and known molecular interactions by IPA were obtained. Thus, several functional groupings of differentially expressed genes were identified. However, this report focused on early events of the bone healing process, including inflammation and angiogenesis, which is most active in the recruitment of cells and release of various cytokines/growth factors, and thus represents a stage of fracture healing.

The up-regulated and down-regulated inflammatory and angiogenesis genes were further examined and revealed some COX-2 related genes, interleukins, growth factors, angiopoietin and VEGF signaling and provided an initial analysis.

The inflammatory and angiogenic genes were significantly up-regulated at 36 h and 3 days after surgery, followed by a down regulation of the genes on day 7, which suggests that inflammatory and angiogenic responses may have been modulated by LLLT (Table 3).

3.2.1.1. Validation of Microarray Data by Real-time PCR. In order to validate the results of the *microarray* assays, the SYBR Green-based real-time PCR on control and irradiated group was performed. The genes

Table 2
Top genetic network.

Network functions	Score
36 h	
Cellular movement, hematological system development and function, immune cell trafficking.	28
Cellular movement, hematological system development and function, hypersensitivity response.	24
Cellular assembly and organization, cellular function and maintenance, cellular movement.	22
Day 3	
Inflammatory response, cellular development, hematological system development and function.	31
Cellular compromise, DNA replication, recombination, and repair, molecular transport.	19
Cellular development, cell cycle, connective tissue development and function.	17
Day 7	
Cellular development, hematological system development and function, hematopoiesis.	26
Cell morphology, tissue development, cellular movement.	24
Cell morphology, cellular assembly and organization, organismal injury and abnormalities.	22

Table 3
List of chosen genes modulated after LLLT irradiation.

Function	Gene symbol	Description	Fold change
36 h			
Inflammation	PTGIR	Prostaglandin I2 (prostacyclin) receptor	1.043
	PTGS-2	Prostaglandin-endoperoxide synthase 2 (prostaglandin G/H synthase and cyclooxygenase)	1.159
	MMD	Monocyte to macrophage differentiation-associated	2.07
	IL-18	Interleukin 18	2.483
	IL-1	Interleukin 1	1.703
Angiogenesis	FGF-14	Fibroblast growth factor 14	2.361
	FGF-2	Fibroblast growth factor 2	3.163
	FGFBP-1	Fibroblast growth factor binding protein 1	2.128
	ANGPT-2	Angiopoietin 2	2.84
Day 3			
Inflammation	PTGER-2	Prostaglandin E receptor 2	3.226
	PTGIR	Prostaglandin I2 (prostacyclin) receptor	−2.322
	IL-4	Interleukin 4	2.899
Angiogenesis	ANGPT-4	Angiopoietin 4	1.098
	PDGFD	Platelet derived growth factor D	1.319
	FGFR-2	Fibroblast growth factor receptor 2	−1.023
Day 7			
Inflammation	PTGFR	Prostaglandin F receptor (FP)	−1.079
	PTGIR	Prostaglandin I2 (prostacyclin) receptor (IP)	−1.815
	PTGS-1	Prostaglandin-endoperoxide synthase 1 (prostaglandin G/H synthase and cyclooxygenase)	−2.738
	IL-18	Interleukin 18 (interferon-gamma-inducing factor)	−2.779
	IL-1	Interleukin 1	−2.564
Angiogenesis	ANGPT-2	Angiopoietin 2	−3.692
	PDGFD	Platelet derived growth factor D	−2.025
	PDGFRA	Platelet-derived growth factor receptor, alpha polypeptide	−3.751

were selected according to the canonical pathway analysis and the references found in previous studies. The expression profiles of the genes confirmed the *microarray* results.

3.3. Immunohistochemistry Analysis

3.3.1. COX-2 Expression

Qualitative immunohistochemical analysis demonstrated that in the first and second experimental periods, COX-2 expression was predominantly detected in granulation tissue for both groups (Fig. 2A). Seven days post-surgery, for CG, the immunoreactivity of COX-2 was mainly observed in granulation tissue. For the LG, COX-2 immunolabeling was observed in granulation and in the osteoblastic cells.

Semi-quantitative analysis revealed a significant increase in COX-2 immunoexpression that was observed in the LG compared to CG, 36 h after surgery. On day 3, no statistical difference was observed between CG and LG. Moreover, COX-2 immunoexpression was higher in CG than in LG on day 7 (Fig. 2B).

3.3.2. VEGF Expression

Qualitative immunohistochemical analysis demonstrated that VEGF expression was predominantly observed in the capillary walls and granulation tissue for both experimental groups 36 h after the surgery. On days 3 and 7 after surgery, the immunoexpression of VEGF was identified in the capillary walls, granulation tissue and osteoblastic cells for both groups (Fig. 3A).

Semi-quantitative analysis demonstrated that VEGF immunoexpression was similar between CG and LG, 36 h after the surgery. On days 3 and 7, LG presented a significantly higher up-regulation of VEGF when compared to the CG (Fig. 3B).

3.4. Discussion

This study aimed to investigate the effects of LLLT on the morphological aspects of a bone callus and on gene and immunomarker expression related to the inflammatory process and angiogenesis during the initial phase of the bone healing process in a model of tibial bone defect in rats.

The main findings showed that LLLT produced an earlier recruitment of inflammatory cells, as well as increased amount of newly formed bone at the site of the injury. Furthermore, our results showed that LLLT produced a significant increase in the expression of genes related to inflammation and angiogenesis. The immunoexpression of COX-2 (36 h) and VEGF (3 and 7 days) was also increased in the laser treated animals.

Increased cell proliferation and acceleration of tissue metabolism are the most important physiological effects of LLLT, which contributes to the stimulation of the healing process after an injury [22]. In this context, several studies demonstrated that LLLT had a positive effect in the process of bone consolidation in experimental models in rats [13,15,23]. Fernandes *et al.* [24] showed that LLLT induced a recruitment of inflammatory cells and increased newly formed bone in the initial phases of bone consolidation. These findings are in line with the results of the current study, whose histological analysis revealed that LLLT improved the biological response of bone tissue by modulating the inflammatory process and stimulating the deposition of newly formed bone at the site of the injury. It seems that LLLT can stimulate osteogenic genes that are involved in bone repair, which may explain the positive results of this therapy on bone healing, with the modulation of the inflammatory process and the earlier recruitment of osteoprogenitor cells, thus increasing the rate of bone formation and bone ingrowth into the defect area [25].

In addition, *microarray* analysis suggests that LLLT could have stimulated the healing process and accelerated the process of bone healing by a down-regulation of pro-inflammatory interleukins (IL1, 1IL6, IL8, IL18) at 36 h after the surgery, followed by up-regulation of anti-inflammatory interleukin (IL4) on day 3. Furthermore, inflammatory cells such as macrophages, neutrophils and fibroblasts are activated to remove damaged tissue and stabilize blood clotting [26]. In the present study, increased activity of monocytes to macrophage differentiation-associated gene (MMD) could be observed, which could be directly related to the up-regulation of prostaglandin genes (PTGIR, PTGS2, Ptger2) which were observed in LG at 36 h and day 3 after surgery, and which may also have contributed to the acceleration of the bone repair observed in the irradiated animals. Specifically in the bone healing process, prostaglandins (PGs) and arachidonic acid products play a key role in the generation of the inflammatory response and the enzyme
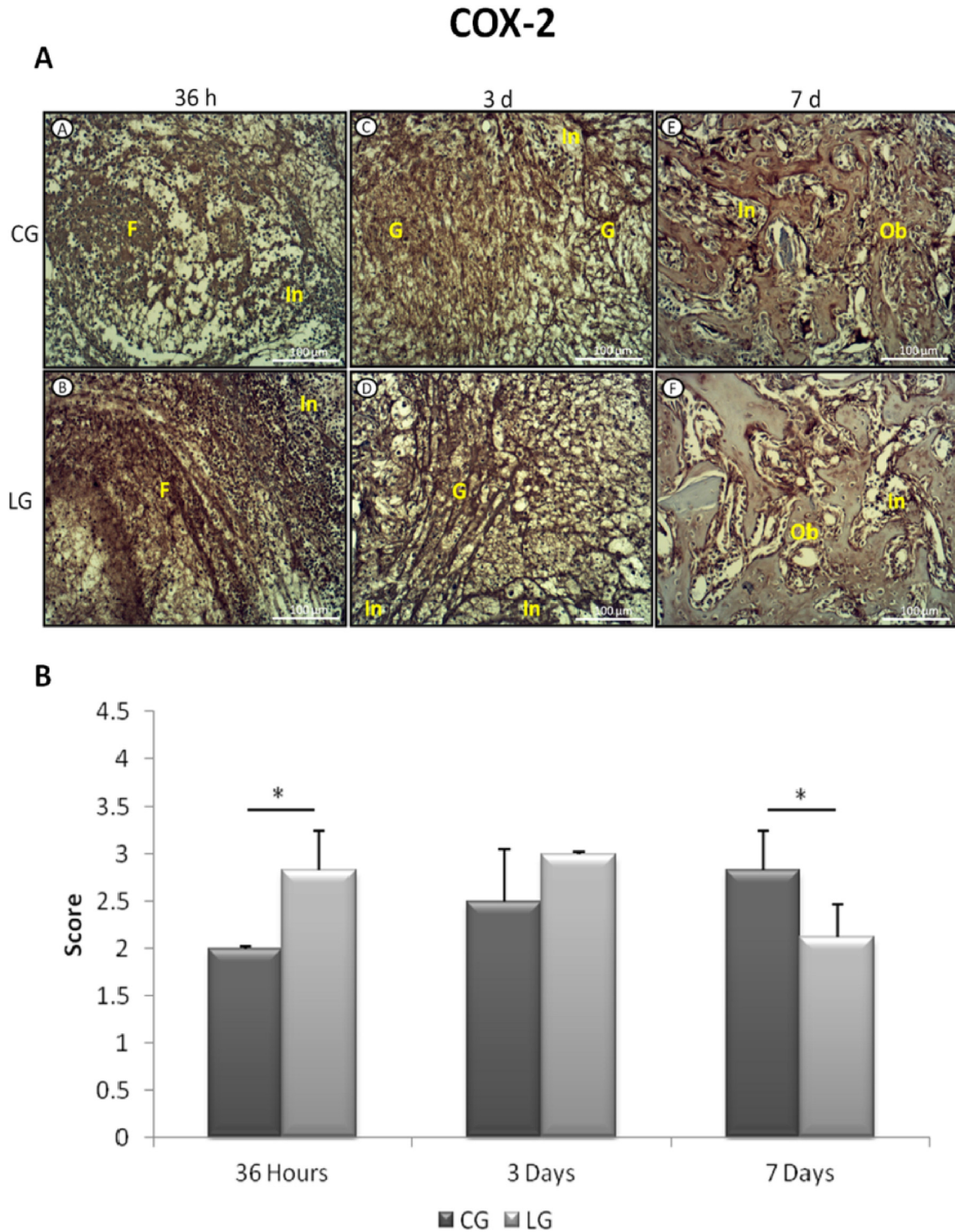
COX-2

Fig. 2. A. Representative sections of COX-2 immunohistochemistry. Fibrin (F), granulation tissue (G), inflammatory infiltrate (In), osteoblastic cells (Ob). B. Means and standard error of the mean of scores immunohistochemistry of COX-2. Significant differences of $p < 0.05$ are represented by a single asterisk (*).

which is responsible for this process (convert arachidonic acid to prostanoids), the cyclo-oxygenase [27]. Additionally, effects of LLLT on the modulation of inflammation were also demonstrated by the increased immunoexpression of COX-2 in the LG in the first experimental period followed by a decreased immunoexpression. These results suggest that LLLT modulates the synthesis of inflammatory mediators which can culminate in the earlier resolution of the inflammatory process observed in the LG, and consequently, may have anticipated the steps of tissue repair, as was demonstrated [28] in histopathological analysis. Some authors have postulated that the early modulation of

pro-inflammatory mediators can prevent excess tissue degradation. This modulation can also stimulate bone repair [13]. There are several reports which highlight LLLT effects on inflammatory modulation [24,29,30]. Recently, Rambo et al., [31] observed that LLLT was effective in decreasing the expression on the pro-inflammatory mediators (IL-1 and TNF) and it was able to increase the expression of the anti-inflammatory cytokine IL-10.

Similarly, angiogenesis is an essential part of fracture repair [32]. Angiogenesis is not only responsible for the oxygen supply, but also a prerequisite for the resorption of necrotic tissue and recruitment of
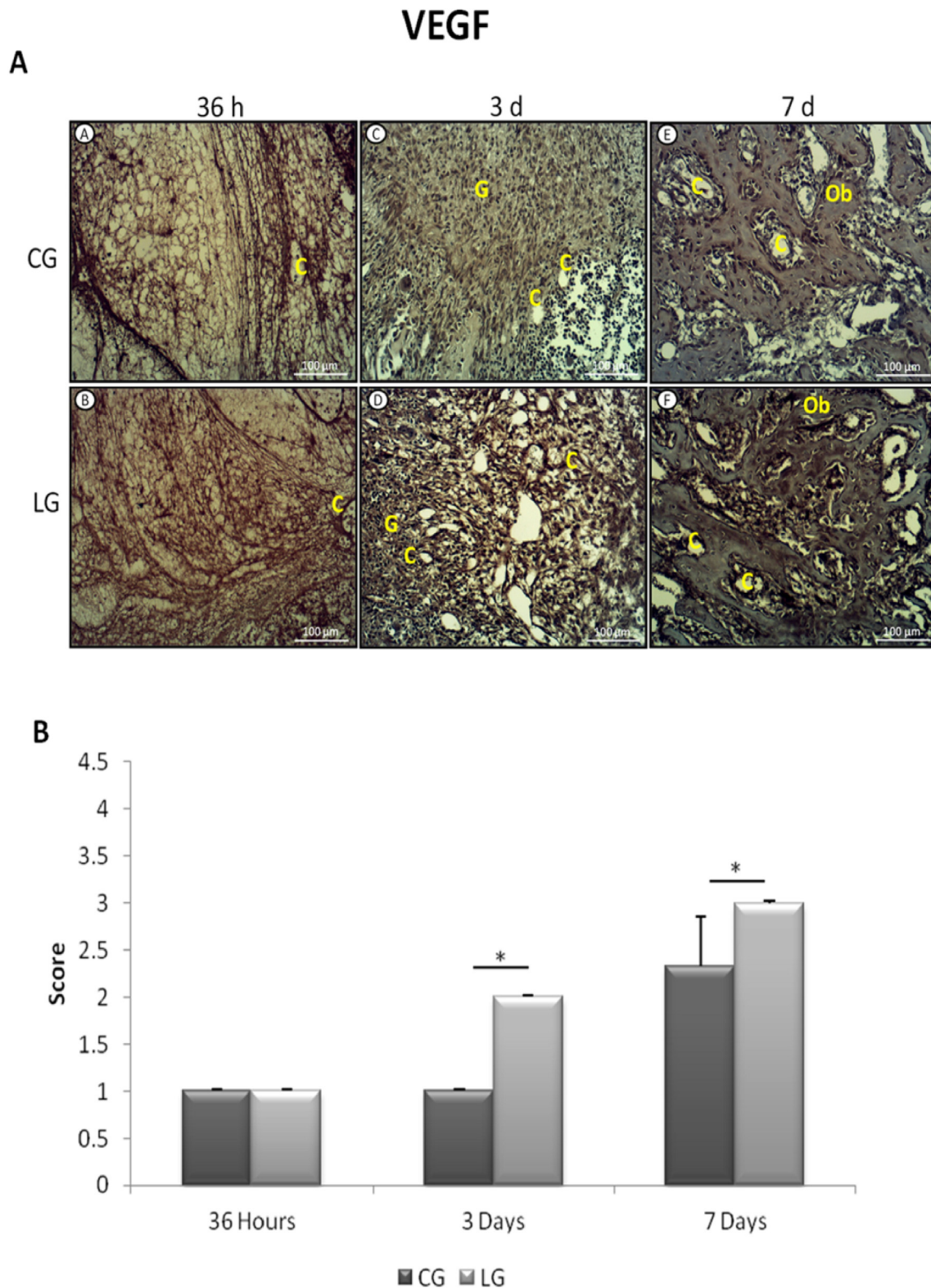
VEGF

Fig. 3. A. Representative sections of VEGF immunohistochemistry. Capillary (C), granulation tissue (G), osteoblastic cells (Ob). B. Means and standard error of the mean of scores immunohistochemistry of VEGF. Significant differences of $p < 0.05$ are represented by a single asterisk (*).

different cell types, such as mesenchymal progenitor cells, which is necessary for a mechanically stable repair of the bone defect. [33]. In essence, FGF and PDGF are required elements in cellular division for fibroblasts, a type of connective tissue cell that is especially prevalent

in wound healing. Also, it has important functions in the promotion of endothelial cell proliferation [34].

In the present study, it was demonstrated that LLLT can stimulate angiogenic genes in injured tissues such as ANGPT2 and ANGPT4, at 36 h

and 3 days after surgery, respectively. In addition, our *microarray* findings showed that LLLT produced an up-regulation of FGF and PDGF at 36 h and 3 days after surgery. Similarly, VEGF immunoexpression was increased after laser stimulation. These results are in agreement with those found by Bossini *et al.*, [13] who investigated the effects of LLLT in osteoporotic rats and concluded that LLLT improves bone repair as a result of stimulation of angiogenesis and newly formed bone.

Taken together, the results of the present study showed that LLLT might be a promising therapy to improve bone consolidation in the initial period of repair by modulating the expression of genes related to inflammation and neoangiogenesis, which may culminate in the stimulation of bone cells and increased newly formed bone. As this study was limited to a short-term evaluation, information on the influence of LLLT on gene expression in long-term analysis still needs to be provided. Also, other molecular pathways such as the expression of genes related to osteoblast differentiation remain to be investigated.

4. Conclusion

This study suggests that LLLT was efficient in modulating the inflammatory process and increasing the newly formed bone. In addition, LLLT produced a significant increase in the expression of genes related to inflammation and angiogenesis. This fact may explain some of the molecular pathways by which LLLT acts on the stimulation of bone tissue during the healing process and results in the earlier resolution of the inflammatory process and earlier differentiation of pre-osteoblastic cells into mature osteoblasts, thus accelerating the bone healing process. Therefore, these data highlight the potential of LLLT to be used as a therapeutic approach for bone regeneration.

Acknowledgments

References

[1] C. Ferguson, E. Alpern, T. Miclau, J.A. Helms, Does adult fracture repair recapitulate embryonic skeletal formation? Mech. Dev. 87 (1999) 57–66.

[2] R. Dimitriou, E. Tsiridis, P.V. Giannoudis, Current concepts of molecular aspects of bone healing, Inj. Int. J. Care Inj. 36 (2005) 1392–1404.

[3] M.E. McGee-Lawrence, D.F. Razidlo, Induction of fully stabilized cortical bone defects to study intramembranous bone regeneration, Osteoporosis and Osteoarthritis, Springer 2015, pp. 183–192.

[4] G. Victoria, B. Petrisor, B. Drew, D. Dick, Bone stimulation for fracture healing: what's all the fuss, Ind. J. Orthop. 43 (2009) 117–120.

[5] A.N. Silva Júnior, A.L.B. Pinheiro, M.G. Oliveira, R. Weismann, L.M. Pedreira Ramalho, R. Amadei Nicolau, Computerized morphometric assessment of the effect of low-level laser therapy on bone repair: an experimental animal study, J. Clin. Laser Med. Surg. 20 (2002) 83–87.

[6] A.S. da Rosa, A.F. dos Santos, M.M. da Silva, G.G. Facco, D.M. Perreira, A.C.A. Alves, L. Junior, E.C. Pinto, P.d.T.C. de Carvalho, Effects of low-level laser therapy at wavelengths of 660 and 808 nm in experimental model of osteoarthritis, Photochem. Photobiol. 88 (2012) 161–166.

[7] T. Karu, Primary and secondary mechanisms of action of visible to near-IR radiation on cells, J. Photochem. Photobiol. B Biol. 49 (1999) 1–17.

[8] D. Hawkins, H. Abrahamse, Effect of multiple exposures of low-level laser therapy on the cellular responses of wounded human skin fibroblasts, Photomed. Laser Ther. 24 (2006) 705–714.

[9] W.-P. Hu, J.-J. Wang, C.-L. Yu, C.-C.E. Lan, G.-S. Chen, H.-S. Yu, Helium–neon laser irradiation stimulates cell proliferation through photostimulatory effects in mitochondria, J. Investig. Dermatol. 127 (2007) 2048–2057.

[10] F.M. de Lima, A.B. Villaverde, M.A. Salgado, H.C. Castro-Faria-Neto, E. Munin, R. Albertini, F. Aimbire, Low intensity laser therapy (LILT) in vivo acts on the neutrophils recruitment and chemokines/cytokines levels in a model of acute pulmonary inflammation induced by aerosol of lipopolysaccharide from *Escherichia coli* in rat, J. Photochem. Photobiol. B Biol. 101 (2010) 271–278.

[11] F.M. de Lima, A.B. Villaverde, R. Albertini, J.C. Corrêa, R.L.P. Carvalho, E. Munin, T. Araújo, J.A. Silva, F. Aimbire, Dual effect of low-level laser therapy (LLLT) on the acute lung inflammation induced by intestinal ischemia and reperfusion: action on anti-and pro-inflammatory cytokines, Lasers Surg. Med. 43 (2011) 410–420.

[12] E.M.S. Laraia, I.S. Silva, D.M. Pereira, F.A. dos Reis, R. Albertini, P. de Almeida, L. Junior, E.C. Pinto, P.d.T.C. de Carvalho, Effect of low-level laser therapy (660 nm) on acute inflammation induced by tenotomy of Achilles tendon in rats, Photochem. Photobiol. 88 (2012) 1546–1550.

[13] P.S. Bossini, A.C.M. Rennó, D.A. Ribeiro, R. Fangel, A.C. Ribeiro, M. de Assis Lahoz, N.A. Parizotto, Low level laser therapy (830 nm) improves bone repair in osteoporotic rats: similar outcomes at two different dosages, Exp. Gerontol. 47 (2012) 136–142.

[14] A.V. Corazza, J. Jorge, C. Kurachi, V.S. Bagnato, Photobiomodulation on the angiogenesis of skin wounds in rats using different light sources, Photomed. Laser Surg. 25 (2007) 102–106.

[15] C.R. Tim, K.N.Z. Pinto, B.R.O. Rossi, K. Fernandes, M.A. Matsumoto, N.A. Parizotto, A.C.M. Rennó, Low-level laser therapy enhances the expression of osteogenic factors during bone repair in rats, Lasers Med. Sci. 29 (2014) 147–156.

[16] L. Assis, A.I.S. Moretti, T.B. Abrahao, V. Cury, H.P. Souza, M.R. Hamblin, N.A. Parizotto, Low-level laser therapy (808 nm) reduces inflammatory response and oxidative stress in rat tibialis anterior muscle after cryolesion, Lasers Surg. Med. 44 (2012) 726–735.

[17] A. Stein, D. Benayahu, L. Maltz, U. Oron, Low-level laser irradiation promotes proliferation and differentiation of human osteoblasts in vitro, Photomed. Laser Ther. 23 (2005) 161–166.

[18] K. Sena, R.M. Leven, K. Mazhar, D.R. Sumner, A.S. Virdi, Early gene response to low-intensity pulsed ultrasound in rat osteoblastic cells, Ultrasound Med. Biol. 31 (2005) 703–708.

[19] Y.A. Vladimirov, A.N. Osipov, G.I. Klebanov, Photobiological principles of therapeutic applications of laser radiation, Biochem. Mosc. 69 (2004) 81–90.

[20] J. Zhao, T. Watanabe, U.K. Bhawal, E. Kubota, Y. Abiko, Transcriptome analysis of β-TCP implanted in dog mandible, Bone 48 (2011) 864–877.

[21] P.A. de Castro, M. Savoldi, D. Bonatto, I. Malavazi, M.H.S. Goldman, A.A. Berretta, G.H. Goldman, Transcriptional profiling of *Saccharomyces cerevisiae* exposed to propolis, BMC Complement. Altern. Med. 12 (2012) 194.

[22] Y.-h. Wu, J. Wang, D.-x. Gong, H.-y. Gu, S.-s. Hu, H. Zhang, Effects of low-level laser irradiation on mesenchymal stem cell proliferation: a microarray analysis, Lasers Med. Sci. 27 (2012) 509–519.

[23] K.R. Fernandes, D.A. Ribeiro, N.C. Rodrigues, C. Tim, A.A. Santos, N.A. Parizotto, H.S. de Araujo, P. Driusso, A.C.M. Rennó, Effects of low-level laser therapy on the expression of osteogenic genes related in the initial stages of bone defects in rats, J. Biomed. Opt. 18 (2013) 038002-038002.

[24] K.P.S. Fernandes, A.N. Alves, F.D. Nunes, N.H.C. Souza, J.A. Silva Jr., S.K. Bussadori, R.A.M. Ferrari, Effect of photobiomodulation on expression of IL-1β in skeletal muscle following acute injury, Lasers Med. Sci. 28 (2013) 1043–1046.

[25] E. Fávaro-Pípi, D.A. Ribeiro, J.U. Ribeiro, P. Bossini, P. Oliveira, N.A. Parizotto, C. Tim, H.S.S. de Araújo, A.C.M. Renno, Low-level laser therapy induces differential expression of osteogenic genes during bone repair in rats, Photomed. Laser Surg. 29 (2011) 311–317.

[26] L.J. Raggatt, M.E. Wullschleger, K.A. Alexander, A.C.K. Wu, S.M. Millard, S. Kaur, M.L. Maugham, L.S. Gregory, R. Steck, A.R. Pettit, Fracture healing via periosteal callus formation requires macrophages for both initiation and progression of early endochondral ossification, Am. J. Pathol. 184 (2014) 3192–3204.

[27] X. Zhang, E.M. Schwarz, D.A. Young, J.E. Puzas, R.N. Rosier, R.J. O'Keefe, Cyclooxygenase-2 regulates mesenchymal cell differentiation into the osteoblast lineage and is critically involved in bone repair, J. Clin. Invest. 109 (2002) 1405–1415.

[28] O. Dortbudak, R. Haas, G. Mailath-Pokorny, Biostimulation of bone marrow cells with a diode soft laser, Clin. Oral Implants Res. 11 (2000) 540–545.

[29] T.Y. Fukuda, M.M. Tanji, S.R. Silva, M.N. Sato, H. Plapler, Infrared low-level diode laser on inflammatory process modulation in mice: pro-and anti-inflammatory cytokines, Lasers Med. Sci. 28 (2013) 1305–1313.

[30] V.S. Hentschke, R.B. Jaenisch, L.A. Schmeing, P.R. Cavinato, L.L. Xavier, P. Dal Lago, Low-level laser therapy improves the inflammatory profile of rats with heart failure, Lasers Med. Sci. 28 (2013) 1007–1016.

[31] C.S. de Melo Rambo, J.A. Silva Jr., A.J. Serra, A.P. Ligeiro, R. de Paula Vieira, R. Albertini, E.C.P. Leal-Junior, P.D.T.C. de Carvalho, Comparative analysis of low-level laser therapy (660 nm) on inflammatory biomarker expression during the skin wound-repair process in young and aged rats, Lasers Med. Sci. 29 (2014) 1723–1733.

[32] J. Street, D. Winter, J.H. Wang, A. Wakai, A. McGuinness, H.P. Redmond, Is human fracture hematoma inherently angiogenic? Clin. Orthop. Relat. Res. (2000) 224–237.

[33] R.A.D. Carano, E.H. Filvaroff, Angiogenesis and bone repair, Drug Discov. Today 8 (2003) 980–989.

[34] J.R. Lieberman, A. Daluiski, T.A. Einhorn, The role of growth factors in the repair of bone, J. Bone Joint Surg. 84 (2002) 1032–1044.